

Damage Characterization of the Z24 Bridge by Transfer Function Pole Migration

R. Andrew Swartz¹, Jerome P. Lynch²

¹*PhD Candidate, Department of Civil and Environmental Engineering,
University of Michigan, Ann Arbor, MI 48109*

²*Assistant Professor, Department of Civil and Environmental Engineering,
University of Michigan, Ann Arbor, MI 48109*

ABSTRACT: In this study, a novel approach to the characterization of structural damage in civil structures is presented. The proposed method is scalable, automated, and well suited to implementation within a low power, low cost wireless sensing network. Structural damage often results in subtle changes to structural stiffness and damping properties that are manifested by changes in the location of transfer function characteristic equation roots (poles) upon the complex plane. Using structural response time-history data collected from an instrumented structure, transfer function poles can be estimated using traditional system identification methods. Comparing the location of poles corresponding to the structure in an unknown structural state to those of the undamaged structure, damage can be accurately identified. Pattern classification methods that have been increasingly popular in recent years for damage detection are leveraged to quantify damage existence, location, and severity. To validate the proposed methodology, response data from the Z24 Bridge is adopted as a test case. Utilization of forced vibration data corresponding to the bridge in various controlled damaged states allow the damage detection methods to be tested; in this study, they are shown to be capable of accurate and robust damage assessment in such a complex civil structure.

TABLE OF NOMENCLATURE:

$y(k), Y(z)$	Output discrete time history value, Z-transformed output.
$u(k), U(z)$	Input discrete time history value, Z-transformed input.
$e(k)$	Output estimation error.
a_i, b_i	Output observation weight, Input observation weight.
$H(z)$	Transfer function.
DI	Damage Index.
Δ_i	Pole cluster mean separation distance.
σ_i	Pole cluster standard deviation.
\mathbf{w}	Perceptron weighting vector.
$bias$	Perceptron bias term.
c	Perceptron correction factor.
θ	Perceptron classification threshold.
η	Perceptron learning rate factor.

1. INTRODUCTION

During their lifetimes, civil structures are subjected to harsh environmental conditions as well as destructive natural and anthropogenic loadings. Any of these phenomena may cause damage and decrease the strength and functional lifespan of the structure. Regular monitoring of civil structures is required to ensure their proper function and the safety of the public that utilizes them. Presently, the most popular means of monitoring is visual inspection. The practice of visual inspection however, has several drawbacks. Certain structural elements are

often difficult for inspectors to access. Additionally, the knowledge of the structural condition garnered during visual inspection is limited to the surface of the structure. Finally, visual inspection is highly subjective. As the recent tragic collapse of the I35W Mississippi River Bridge in Minneapolis, MN demonstrates, regular visual inspections do not guarantee that fatal problems will be detected. The I35W Bridge collapsed August 1st 2007 during rush hour killing 13 motorists. The bridge, classified as "structurally deficient" during annual visual inspections, was still considered to be safe for continued operation [1]. In light of this and other collapses, researchers are investigating the application of structural health monitoring techniques to civil infrastructure systems. Equipped with an automated, embedded health monitoring system, structures can monitor and report changes in their conditions to authorities before catastrophes can occur.

Structural health monitoring can be characterized as a five step process in which the ultimate goal is to answer questions regarding existence, location, type, and severity of damage, as well as estimate the remaining useful structural lifespan [2]. Intrinsic to the structural health monitoring process is a definition of damage. A common definition is a change in structural behavior that is detrimental to the structure's ability to perform its intended function. Such behavior of a civil structural system can be characterized using vibration data. Comparing this behavior to a model of the behavior of the healthy structure can help to answer the five structural health monitoring questions. Reviews of structural health monitoring techniques have been compiled by Doebbling, *et al.* [3] and Sohn, *et al.* [4]. Ideally, a dense network of sensors is available to collect vibrational data. With wiring costs exceeding \$1000 per sensing channel in large civil structures [5], wireless sensing networks become a more economical platform for health monitoring than do traditional cable-based sensor networks [6, 7]. Low power, low cost systems can be easily installed and require little maintenance. Wireless networks do have two associated challenges however: limited power resources (e.g. finite battery lives) and limited available bandwidth for communications. Collocating sensors and low power microprocessors means that data interrogation can reduce the network's dependence on data transmissions thereby preserving bandwidth and power [6].

In this paper, a novel signal processing technique for structural health monitoring of civil structures suitable for use in an automated wireless sensing network is presented using the Z24 Bridge as a testbed. Dynamic data for a large number of damage cases is available for the Z24 Bridge from the System Identification to Monitor Civil Engineering Structures (SIMCES) project. In 1998, the Z24 Bridge located between Utzenstorf and Koppigen in Switzerland was heavily instrumented and monitored as it was progressively damaged to provide researchers with vibrational data corresponding to the progressive damage levels. The bridge is a three span bridge with exterior spans of 14 m each and a center span of 30 m with concrete piers between. The bridge is constructed using prestressed, two-cell box girders with tendons located in the webs of the girder. A description of the SIMCES Z24 Bridge project is available by De Roeck, *et al.* [8] with a description of the progressive damage states provided by Krämer, *et al.* [9]. Peeters and Ventura [10] have compiled a comparison of several modal analysis techniques employed on the Z24 bridge data set including peak picking [11], frequency domain decomposition (FDD) [12], rational fraction polynomial [13], ARMA two-stage least squares [14], and subspace identification [12, 15]. A number of health monitoring methods have also been proposed using the Z24 Bridge data set for validation including finite element model updating [16-17], control charts [18], modal frequencies and shapes [19], and subspace identification models [20]. Intrinsic in these methods is the assumption that a centralized data server is available for data archival and processing. In wireless sensor networks, distributed data processing is preferred in order to avoid unnecessary and power draining transmission of raw data from every sensor in the network [6].

The method presented herein consists of three parts. First, an autoregressive with exogenous input (ARX) algorithm is used to take input/output time history data, calculate ARX coefficients, and then convert those coefficients to system poles. Second, a sorting algorithm that matches the identified system poles with the appropriate baseline pole cluster is adopted. Last, a health monitoring algorithm that calculates damage using a damage index based on system pole locations is proposed. System poles are useful for health monitoring as they encapsulate information regarding natural frequencies and damping ratios of the measured system [21, 22]. The damage index calculated is intended to represent an analytical assessment of the health of the monitored system. The first two steps are repeated to generate clusters of poles for each test case. The method proposed in this study is well suited to distributed, automated networks of wireless sensors because it allows individual sensing nodes within the network to do the bulk of their computations using their locally measured output. Once the ARX models are computed on the individual nodes, they sort the poles and calculate their own damage index terms individually. Only in the final step do the sensors need to transmit to the network to collectively choose the final damage index and decide if an alarm is warranted. By deciding on the final estimation of the state (damaged

versus undamaged) of the monitored system collectively and using a number of pole clusters, the network reduces the likelihood that an anomaly in the signal recorded by a single unit (or at a single frequency) will trigger a false alarm.

The structure of the paper is as follows. First, the theory behind ARX time-series modeling and its relationship to system poles are presented. Next, three classifiers of system poles designed to measure their movement over time are developed followed by a system for integrating damage assessment results from multiple classifiers, multiple poles, and multiple sensing nodes. The methods section describes how the Z24 Bridge progressive test data was utilized, the progressive damage tests themselves, and provides a description of the modeling and sorting methods used. Next, modal and health monitoring results are presented, followed by concluding remarks and suggestions for future work.

2. THEORY

For linear, time-invariant (LTI) systems, a number of mathematical tools exist to characterize the relationship between inputs to the system and measured outputs. One simple model is the linear difference equation that consists of n weighted observations of the input to the system, $u(k)$, and m weighted observations of the output to the system, $y(k)$:

$$y(k) + a_1 y(k-1) + \dots + a_m y(k-m) = b_0 u(k) + b_1 u(k-1) + \dots + b_n u(k-n) + e(k) \quad (1)$$

In cases where b_0 is not equal to zero, the difference equation includes a direct transmission term. Rearranging (1), an estimate of the k th output can be calculated:

$$\hat{y}(k) = -a_1 y(k-1) - \dots - a_m y(k-m) + b_0 u(k) + b_1 u(k-1) + \dots + b_n u(k-n) \quad (2)$$

rendering $e(k)$ of (1) the error between the measured output and the estimated output from the model [23]. The linear difference equation in this form is an ARX time-series model. The ARX model is computationally simple, making it well suited for embedded wireless sensor applications. A straightforward least-squares algorithm or recursive filter may be used to fit an ARX model to a set of training data identifying the a and b coefficient values [23]. Converting the linear difference equation into a transfer function is accomplished by taking its Z-transform. The Z-transform is described by:

$$F(z) = \sum_{k=-\infty}^{\infty} f[k]z^{-k} \quad (3)$$

In the z-domain, the LTI transfer function, $H(z)$, derived from the Z-transform of the ARX model describes the response of the system to a unit impulse input. For the ARX model, the transfer function is:

$$H(z) = \frac{Y(z)}{U(z)} = \frac{b_0 z + b_1 z^{-1} + \dots + b_n z^{-n}}{1 + a_1 z^{-1} + \dots + a_m z^{-m}} \quad (4)$$

The roots of the numerator of $H(z)$ are the locations in the complex z-plane (Figure 1) at which the transfer function equals zero, rendering them the “zeros” of the system. Similarly, the roots of the denominator define the locations in the complex z-plane at which the transfer function approaches infinity making those z values the “poles” of the system. The locations of the zeros of the system are defined by properties that relate the system input to the system output, however the locations of the poles are defined by properties of the entire system and are independent of the choice made for input and output. A change in the locations of the system poles can be interpreted to indicate a physical change in the system that might be due to damage. The number of poles is equal to m and is determined by the number of past observations of the output included in the model. Similarly, the number of zeros is equal to n and is determined by the number of past observations of the input included in the model.

The location of system poles on the complex z-plane yields useful information regarding the properties of the system. A system whose poles are all located within the unit circle is stable in the sense that any bounded input applied to the system will result in a bounded output. Furthermore, contour lines of constant frequency and

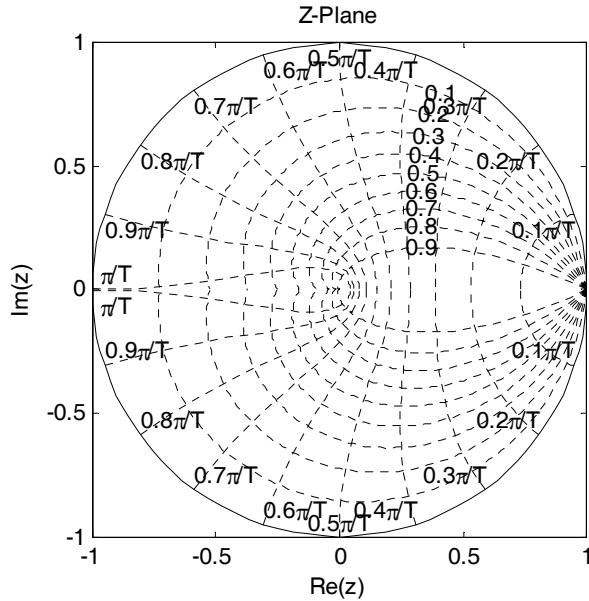


Figure 1: The complex z-plane.

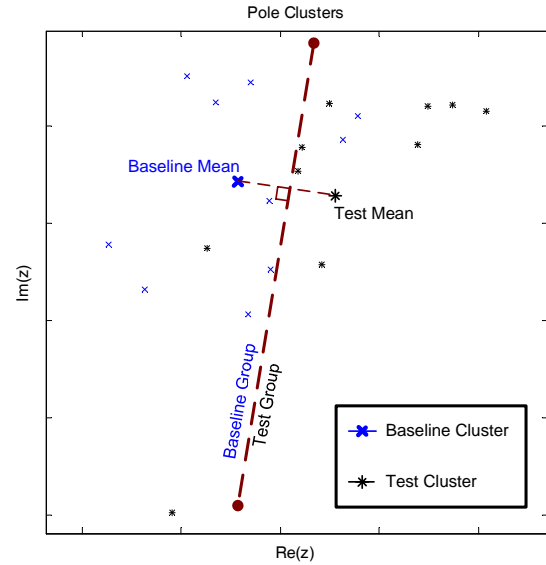


Figure 2: Nearest mean classification (note in this example, two baseline and one test pole misclassified).

damping may be drawn on the z-plane (as shown in Figure 1) illuminating the fact that, not only is the location of a system pole indicative of the frequency on a particular mode of the system, but it is also an indication of its damping ratio. This fact means that in identifying the pole location, two parameters of the system are known, namely frequency and damping. Having two parameters available makes system pole identification a more powerful damage detection technique than those that rely on frequency alone. As damage to the structure has an increased effect on the vibrational characteristics of the structure, the system poles defined by the linearly fit model will change their locations on the complex plane.

2.1 Nearest mean classification

The first component of the damage index is based on a very simple classifier of the poles. As data is collected, clusters of poles are identified and compared with pole clusters identified from the undamaged baseline state. The mean z values of the baseline and test pole clusters are then computed. Poles are classified into one of two groups, one group that is nearest the mean z value calculated for the undamaged state and one group that is nearer the test mean value. As more poles are incorrectly classified, the two pole clusters are less separable and hence, the difference between the test data and the baseline data is smaller. This fact in turn reduces the likelihood that the structure is damaged. In Figure 2 the nearest mean classifier is illustrated demonstrating that the boundary between the two sets of poles, as classified, is defined by a straight line perpendicular to the line connecting the cluster means. The contribution to the damage index is:

$$DI_{nearest} = \frac{\text{Number Correctly Classified Poles}}{\text{Total Number Poles per Cluster}} \quad (5)$$

where the number of correctly classified poles is normalized by the total number of poles in a cluster. This damage index is naturally normalized to vary between zero (in the case of no correctly separated poles) and one (in the case of all poles correctly separated).

2.2 Perceptron classification

The second means of classifying system poles involves use of the perceptron criterion function. A perceptron is a linear classifier capable of correctly separating and classifying the members of linearly separable groups. For a two parameter system, the perceptron will correctly classify two groups of points that can be divided by a straight

line. Unlike the nearest mean classifier however, the classifier algorithm has additional freedom in placing the location of that line. A perceptron may also be thought of as a single neuron that might be used in a more complicated neural network. The contribution to the damage index from the perceptron classification method is again based on the number of correctly classified poles. Use of a fixed-increment, single-sample perceptron guarantees convergence on a solution as opposed to the batch perceptron, for which no such guarantee exists [24]. In the fixed-increment, single-sample approach, the algorithm computes the dot product of the coordinate vector for each pole and a weighting vector, \mathbf{w} , and adds that result to a bias term. If the resulting value exceeds the classification threshold, the pole is classified in one group, if not, then the other. When a pole is misclassified, the algorithm alters the weighting vector and bias value by an amount equal to the classification error times a learning constant, η . The algorithm continues for a predefined number of iterations through the data set or until no misclassifications are found. For a more detailed description of the algorithm used to determine a linear decision boundary for a perceptron classifier, interested readers are referenced to [24]. The contribution to the damage index from the perceptron classification method is based on the number of incorrectly classified poles. The damage index term is:

$$DI_{\text{perceptron}} = 1.0 - 2.0 * \left(\frac{\text{Number Incorrectly Classified Poles}}{\text{Total Number Poles}} \right) \quad (6)$$

where the term in parentheses varies between {0.0, 0.5} meaning that there is an upper limit of one half to the number of poles that will be misclassified using the perceptron. Figure 3 depicts the perceptron classified on the z-plane.

2.3 Mean separation distance criterion

The first two components of the damage index are based upon the abilities of two rudimentary linear classifiers to correctly separate clusters of poles identified from data collected from the healthy and unknown-state structures. As damage to the structure affects its vibration properties and causes the locations of the pole clusters to deviate, this separation becomes easier to detect when the poles remain well clustered. These methods lose their abilities to discern changes to the structure once the pole clusters become perfectly separable. As the mean distance between the pole clusters increases, there is no corresponding increase in damage index value if the number of misclassified poles is already equal to zero. To address this fact, an additional component of the damage index is developed that accounts for the separation distance between the cluster means. The separation distance classifier takes the distance between the cluster means and then normalized it by the test cluster standard deviation along the line connecting those means (Figure 4). Here, a 2-dimensional Gaussian distribution is fit to the set of poles in the cluster; as shown in Figure 4, the first level curves are shown for each cluster distribution. The damage index term is:

$$DI_{\text{distance}} = \frac{\Delta_i}{\sigma_i} \quad (7)$$

where Δ_i is the i^{th} pole cluster mean separation difference and σ_i is the i^{th} pole cluster standard deviation in the direction of the line between the cluster means. Because the mean separation distance may be arbitrarily large compared to the standard deviation of the pole cluster distribution, this damage index term is not naturally bounded or normalized to one as are the previous two terms. Normalization of this term is accomplished empirically for the structure of interest during the aggregation step described in the following section.

2.4 Aggregation of classifiers

A wireless network employing a damage detection algorithm based on the classifiers described above would have to generate ARX models, locate their poles, and calculate damage index terms. Next, the wireless sensors would require a rational means for combining the results from all three classifiers. Not only that, the network would then have to combine the results from every pole cluster considered in the model and integrate the results from every sensor in the network. Two separate approaches are used to combine the results: an approach similar to AdaBoosting [24] is utilized to give weights to the resulting damage indices obtained from the three classifiers to combine the results into a single damage index. As will be described, the damage indices from every pole cluster and sensor are normalized to the magnitude of the operational deflection shape calculated for each modal frequency.

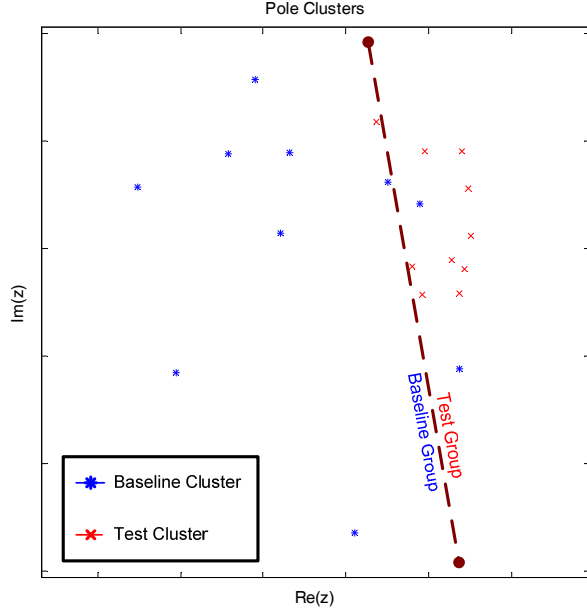


Figure 3: Perceptron classification (note in this example, two baseline and one test pole misclassified).

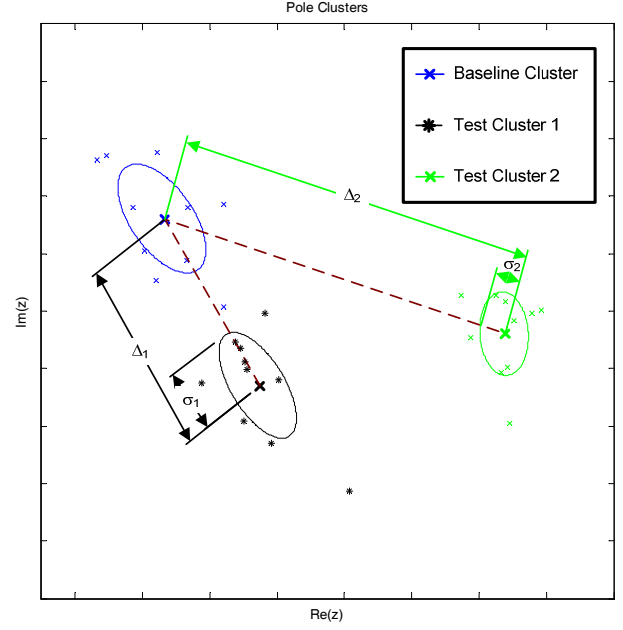


Figure 4: Mean separation distance criterion.

In AdaBoosting, the training data set is repeatedly classified using the available classifiers generating weighting functions based on the success or failure of a particular classifier in properly separating data sets, in this case, test and baseline structural vibration data. Under AdaBoosting, each classifier need be only a weak learner, having results only slightly better than chance, in order to be valuable to the ensemble [24]. Due to the limited number of poles that can be generated from the available Z24 data, the training data set is rather limited making the formal AdaBoost algorithm difficult to apply. Instead, weights for the damage index terms are selected manually that result in the best possible discrimination of each term between damaged and undamaged cases. Weights are selected that normalize damage index terms to be less than one for undamaged cases, and more than one for damaged cases. It is in this step that the mean separation distance damage index term is empirically normalized.

In order to combine results by pole and by sensor, operational deflection shapes are calculated from the undamaged modeling data set. Averaged Fast Fourier Transforms (FFT) of the input and the output data are computed and the transfer function is formed. Taking the imaginary portion of the transfer function at a given modal frequency yields the operational deflection shape of the structure. Assuming broadband excitation of the structure, the operational deflection shape can be said to be the same as the mode shape. Operational deflection shapes provide a rough measure of the level of response at each sensor location for a given mode. Therefore, it will be an ideal tool for weighting the contribution of the damage indices at a given sensor and mode. In this way, information observed by a sensor from an identified mode of the structure will be heavily weighted if that sensor is on a very active part of the mode shape. Similarly, if the sensor is at or near a zero node of the mode, information regarding the movement of that mode's poles will be given very little weight. The operational deflection shapes are all normalized to a peak value of one. The final equation for calculation of the damage index (DI) is:

$$DI = \frac{1}{N} \sum_{i=1}^N \left[\frac{1}{M} \sum_{k=1}^M w_{ModeShape(k)} \left(\frac{DI_{nearest(i,k)}}{w_{nearest}} + \frac{DI_{perceptron(i,k)}}{w_{perceptron}} + \frac{DI_{distance(i,k)}}{w_{distance}} \right) \right] \quad (8)$$

where N is the number of sensors in the network, M is the number of poles used in the ARX model, $w_{nearest}$, $w_{perceptron}$, and $w_{distance}$ are the weights placed on the nearest mean, perceptron, and mean separation distance terms respectively, and $w_{ModeShape}$ is the operational deflection shape value used as a weight placed on the resulting damage index terms for a given sensor location and pole.

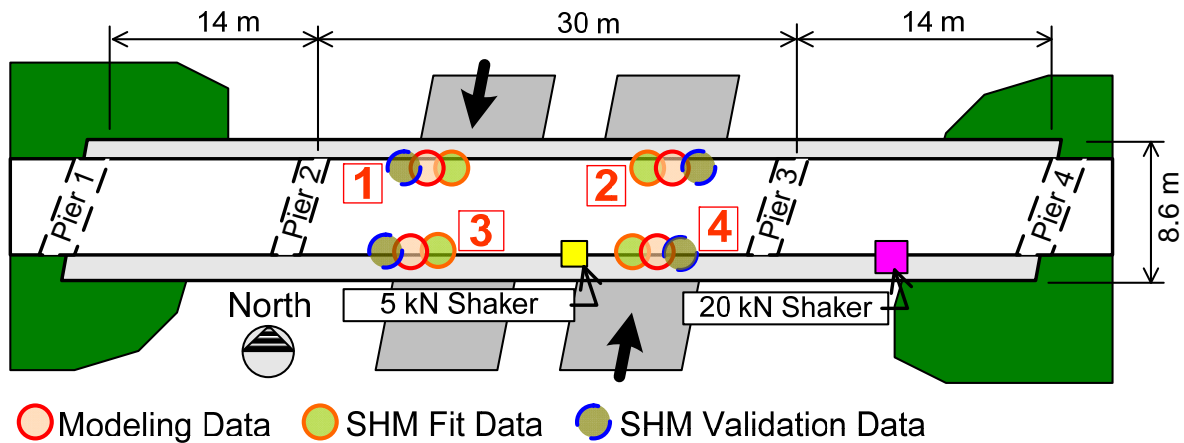


Figure 5: Sensor Layout of accelerometers on the Z24 bridge.

3 METHODS

The best practice for system identification requires division of the data into fit and validation sets. The fit set is used to build the model and choose its size. The validation set is then used to check the veracity of the model against new data to help avoid over fitting the data and its noise. Furthermore, the health monitoring aspect of this study requires additional data once the model size and structure has been determined. One set of data is required to choose weights for the damage index terms and another set of data is required to test those weights to determine their effectiveness in blindly separating damaged cases from undamaged cases. In this study, sensor data is taken from four locations located near the center of the span and along the edges of the bridge. Because the bridge is very densely instrumented, accelerometers are very close together: 1.5 m apart. During each test, 65,536 data points are collected from each sensor. To allow for 10 poles per cluster and an adequate number of data points to fit per pole, adjacent accelerometers are considered to be located at approximately the same location. This practice allows for the use of the entire time history from a sensor location for modeling. Then an adjacent sensor may be used to fit the damage index terms. Finally, a third sensor provides the final validation data for the health monitoring application. The locations of the sensors on the Z24 Bridge are depicted in Figure 5.

3.1 Z24 Bridge progressive damage tests

The Z24 Bridge progressive damage tests offer an unprecedented opportunity for comparison of the vibrational characteristics of a single structure under a wide array of damage and distress conditions. The bridge is heavily instrumented with accelerometers and excited vertically by the use of two hydraulic shakers located on the bridge deck, the first being a SCHENK POKK/N capable of producing forces between ± 5 kN in a frequency band between 2.3 and 100 Hz; the second shaker is a SCHENK PLz 25 N Q 160 capable of generating ± 20 kN between 1.5 and 60 Hz. Both shakers were configured to output random, broadband signals. HBM C2 force transducers were available to record the force imparted by the shakers to the structure. The force signal is taken as the input to the system. The outputs considered are vertical accelerations of the deck. The sampling rate used is 100 Hz.

Progressive damage tests are executed strategically with reversible and less extensive forms of damage inflicted on the structure first, and more extensive, irreversible damage inflicted on the structure later. First, a hinge is added in one pier (Pier 3) to facilitate reversible damage of the form of pier foundation settlement or rotation. This case is regarded as the baseline case to which the other progressive damage cases are compared. Following the installation of the hinge, the pier is progressively lowered by 20 mm, 40 mm, 80 mm, and 95 mm. Audible and visible cracking is observed between the 40 mm level and the 80 mm level with additional cracking occurring between the 80 mm and 95 mm levels. Once the pier is restored, the footing is rotated resulting in a 15 mm differential settlement from one side to the other. Upon completion of these progressive damage tests, the pier is restored to its original position and the irreversible damage tests are undertaken. Spalling of concrete and a landslide at the East abutment are simulated, followed by a cut in the concrete connection between one pier

Table 1: Description of progressive damage tests.

Test Number	Description (Reversible Damage)	Test Number	Description (Irreversible Damage)
1	No Damage	9	Concrete Spalling: 12 m ²
2	No Damage, Pier Hinge Added (Baseline)	10	Concrete Spalling: 24 m ²
3	Pier Settlement: 20 mm	11	Landslide at Abutment
4	Pier Settlement: 40 mm	12	Concrete Hinge Failure
5	Pier Settlement: 80 mm	13	Anchor Head Failure (2)
6	Pier Settlement: 95 mm	14	Anchor Head Failure (4)
7	Pier Foundation Tilt	15	Tendon Wire Failure (54/2)
8	No Damage, Pier Restored	16	Tendon Wire Failure (100/4)

column and the box girder to simulate a concrete hinge failure (Pier 4). Finally, the pretension system is attacked by destroying 2 and then 4 anchor heads, and then with 2 and 4 tendons (54 and 100 wires respectively) cut. A summary of the 16 progressive damage tests may be found in Table 1 [9]. A seventeenth test is undertaken in which 6 pretension tendons (154 wires) are cut, however, the data from those tests are not currently available to the authors of this study.

Of particular interest are progressive damage tests 5 and 6 in which the pier settlement is greatest. Besides the audible and visual cracking reported during the lowering of the pier to these points, noticeable changes in the eigenvalues of the system are observed between these cases and the baseline case. Previous studies of the Z24 Bridge data set using more computationally intensive algorithms have demonstrated that these damage cases are very detectable [16-20] so the method presented in this study must also be able to detect damage for these cases in order to have merit.

3.2 Modeling

The modeling data set is taken from the baseline set (progressive damage test 2) and is divided in half with the first half used to build ARX models of increasing sizes and the second half reserved as validation data to confirm the model size. ARX models are automatically fit for m and n ranging from 2 to 100 and the resulting transfer function compared to the experimental transfer function from the validation data set in the frequency domain. During the course of the investigation, models with direct transmission terms where m and n are equal produce the lowest mean-squared (LMS) error between theoretical and experimental transfer functions. Plotting the LMS error versus model size yields Figure 6. Ultimately, a 60 pole, 60 zero model is selected. The transfer function comparison is presented in Figure 7. Because the structure is excited simultaneously by two shakers, a multiple input single output (MISO) least squares ARX model is fit to the input data and each single-node output.

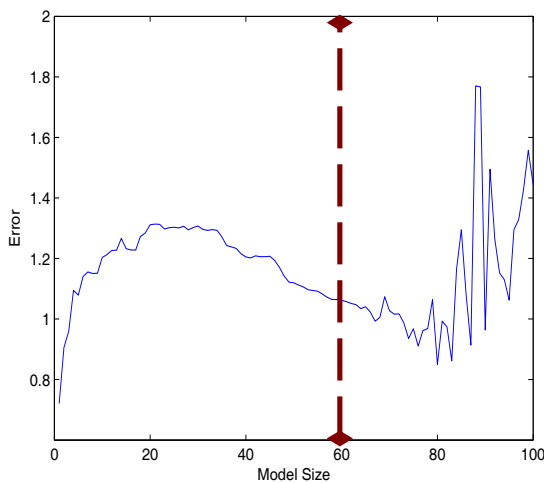


Figure 6: Frequency domain error versus ARX model size.

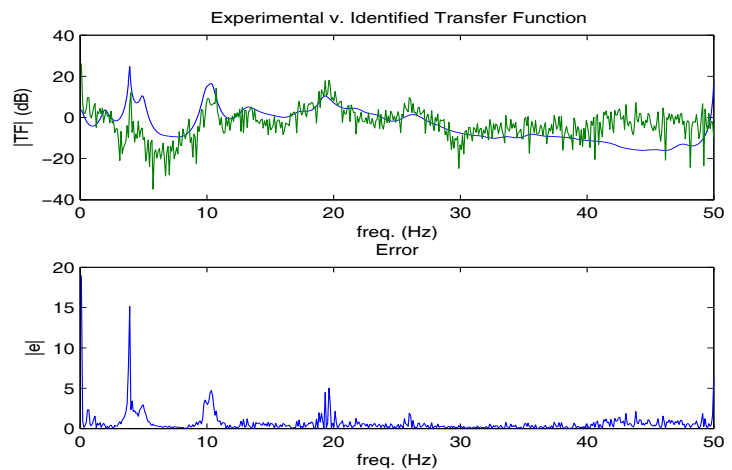


Figure 7: Experimental and identified transfer functions.

Table 2: List of Eigen frequencies of baseline poles used in health monitoring algorithm.

Mode Number	Modal Frequency (Hz)	Identified in Peeters and Ventura [10]?
1	1.97	
2	3.88	Yes
3	4.94	Yes
4	7.22	
5	9.78	Yes
6	10.27	Yes
7	12.62	Yes
8	13.66	Yes
9	15.68	
10	17.34	Yes
11	19.29	Yes
12	19.87	Yes

Poles that are highly consistent in their locations are most useful for automated health monitoring. For a structure of this type, this fact makes less desirable poles that the algorithm places on the real axis as well as higher order poles. Analysis of the baseline data from a number of sensors demonstrated that the ARX algorithm occasionally placed pairs of poles on the real axis. The health monitoring algorithm is programmed to ignore those poles. The remaining poles occur as complex conjugate pairs and are distributed around (and inside of) the unit circle. Additionally, higher order poles are found to cluster poorly, exhibiting much larger deviations than lower order poles and therefore, are not used by the health monitoring algorithm. Once ARX models are assembled for the test cases, the identified poles must be automatically sorted. The sorting is accomplished by a sorting algorithm that minimizes the LMS error or the distance between a set of poles and the baseline means. When a set of 60 poles is generated, the sorting algorithm first discards any poles on or below the real axis (poles below the real axis are redundant). Then it searches every ordered list of the remaining poles, looking for the permutation that yields the smallest LMS error of the distance between poles one through twelve. This process is repeated ten times for every progressive damage test yielding twelve pole clusters composed of ten poles each. These pole clusters are then run through the health monitoring algorithm described in Section 2 to generate damage indexes that automatically separate cases with detectable damage from cases without.

4. RESULTS

The first twelve pairs (with the lowest eigenvalue) of poles identified by the automated ARX algorithm are selected for structural health monitoring and are summarized in Table 2. The mean pole location for the baseline cluster defines the location of these poles. These poles have modal frequencies ranging from 1.97 to 19.87 Hz; nine of these poles are identified in the comparative study of modal analysis techniques for the Z24 Bridge conducted by Peeters and Ventura [10]. Pole clusters along with first standard deviation level curves are presented for the twelve baseline poles in Figure 8. The operation deflection shapes at the sensor locations for the twelve poles of interest are calculated. Figure 9 plots the relative weight given each frequency at each sensor location based on these operational deflection shapes.

Movement of pole clusters can be observed qualitatively as the damage tests progress. First, looking at the reversible progressive damage tests (Figure 10a, 10d, and 10g) and focusing on the closely spaced pole clusters 5 and 6, small changes can be observed in the pole locations between tests 2-4. Larger movement is observed for tests 5 and 6 with the pole clusters returning back near the original baseline location during tests 7 and 8. Second, looking at the irreversible progressive tests (Figure 10b-c, 10e-f, and 10h-i) and again focusing on pole clusters 5 and 6, shows less overall movement of the pole clusters as the damage tests progress but a discernable jump is observed during damage case 12 with future progressive damage tests yielding pole clusters centered close to this new location.

Applying the damage index provides a quantitative assessment of pole movement during the damage test cases. Taken by itself, the nearest mean classifier shows some variation between the baseline case and the tests that are damaged; the resulting combined damage index terms for progressive damage tests 2-16 are presented (normalized by operational deflection shape, number of poles used, and number of units) in Figure 11(a). The perceptron classifier shows better discernment between undamaged and damaged cases; Figure 11(b) presents the combined perceptron classifier damage index term. The mean separation distance criterion shows a very

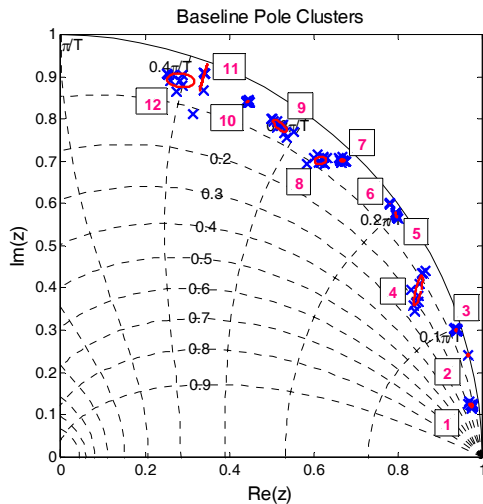


Figure 8: Baseline pole clusters for SHM.

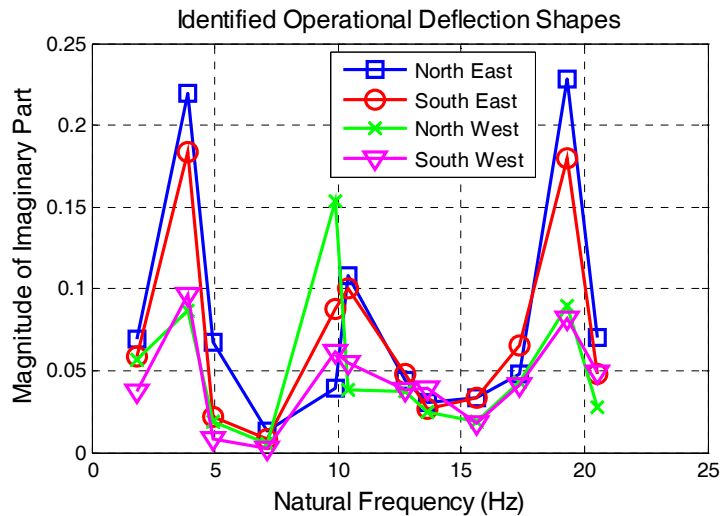


Figure 9: Identified operational deflection shapes.

large discrepancy between the poles of tests 5 and 6 and the rest of the tests. This result can be seen in Figure 11(c). Weighting values are manually selected to combine the results of the three damage index terms. The nearest mean classifier term is multiplied by 7.2, the perceptron classifier term is multiplied by 4.0 and the mean separation distance term is multiplied by 4.0. Added together, these terms yield the final damage index, Figure 11(d). Higher damage index values suggest a greater probability of damage. Here, progressive damage tests 5 and 6 show very high damage indices indicating very high probability of damage where tests 7 and 12 (and all subsequent tests) show elevated damage indices indicating an increased probability of damage. The vibrational properties of the restored pier (test 8), as measured by the damage index, appear to be quite similar to the original baseline properties. It also appears that there is very little change in the linear behavior of the system after test 12.

5. Conclusions

This paper presents a simple set of algorithms for health monitoring of civil structures that is suitable for distributed implementation within a wireless sensing network. Basing the damage detection algorithm on the locations of system poles in the z -plane gives the network information about not only changes in frequency, but also damping of the monitored structure. By taking into account both the input and the output to the system, variability in the pole locations due to inconsistent excitation can be significantly reduced over output-only or ambient monitoring methods. A high-order ARX model (60 poles and 60 zeros) produces poles that are consistent enough that an automated sorting algorithm can properly form pole clusters for the first 12 modal frequencies that are the basis of the health monitoring algorithm. The drawback however, is that this method, in its current incarnation, is limited to systems in which a measurable input is available.

Because the outputs are never transmitted, the amount of raw data transmissions that are necessary between nodes in the wireless network is limited. This monitoring method addresses the two most problematic limitations of wireless sensing networks: limited bandwidth for communications and the high power drain of the limited battery supplies incurred during wireless transmissions. The wireless nodes are free to do most of their computations independently of the network and only conferring to produce the final damage index value that would potentially trigger the alarm. The method is found to be effective in detecting damage due to large settlement of the pier (progressive damage tests 5 and 6) with the restored pier pole locations returning to their baseline locations (progressive damage test 8), as well as concrete hinge failure (progressive damage test 12). Detection of the remaining progressive damage tests proved to be more challenging.

Future work should concentrate on developing an automated output-only approach that remains computationally efficient with limited transmission of data between sensor nodes. An output-only algorithm frees the sensing network of its reliance on a known input excitation source and also frees the network of the need to transmit input data to the sensing nodes. This study neglects the positions of the zeros of the system which are less dependent

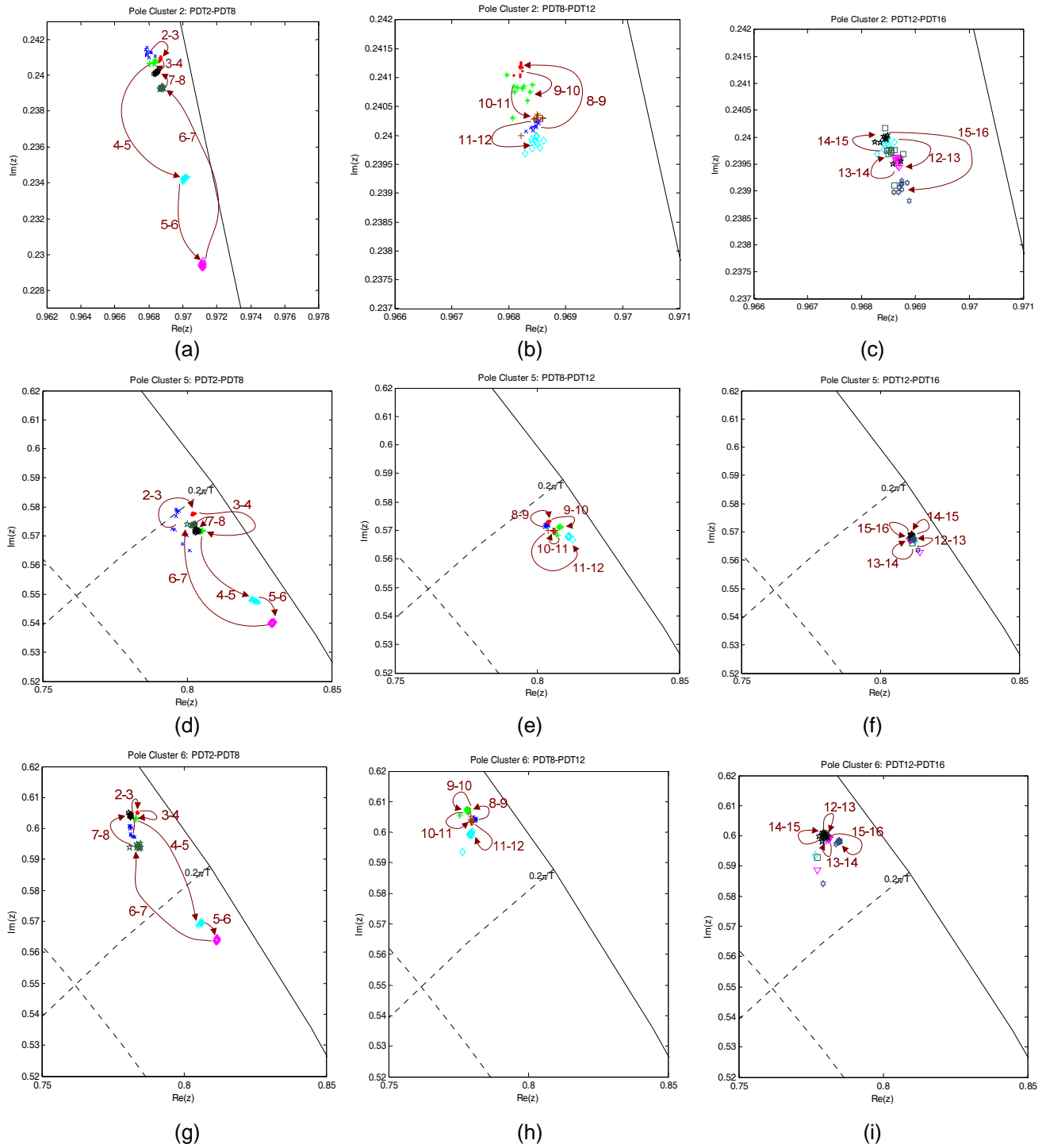


Figure 10: Sample pole clusters at Pole Cluster 2 (a-c), Pole Cluster 5 (d-f), and Pole Cluster 6 (g-i).

on the behavior of the system as a whole and are more dependent upon the relationship between the input and the output at a specific location. If the system zeros can be calculated and sorted in a sufficiently consistent manner, they may yield a redundant check on the structural condition assessment found by analysis of the poles as well as information regarding the location of identified damage. Finally, integration of the environmental monitoring portion of the Z24 Bridge monitoring project with the data from the progressive damage tests may yield a relationship between environmental factors and movement of the system poles that should be accounted for in future damage detection studies.

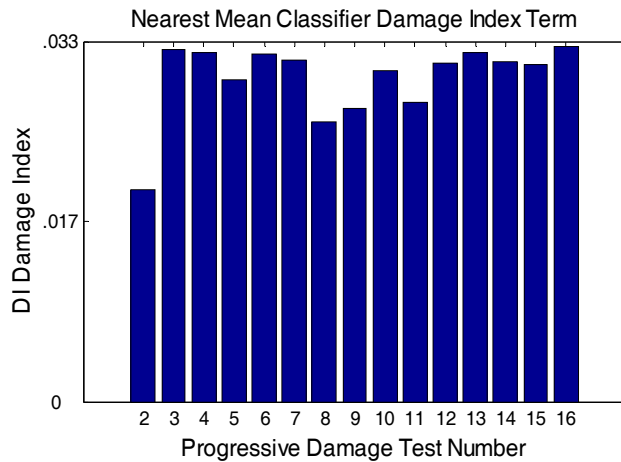


Figure 11(a): Damage index contributions from the nearest mean classifier.

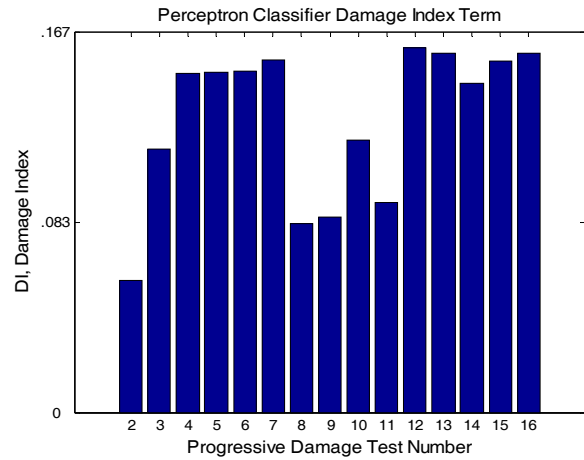


Figure 11(b): Damage index contributions from the perceptron classifier.

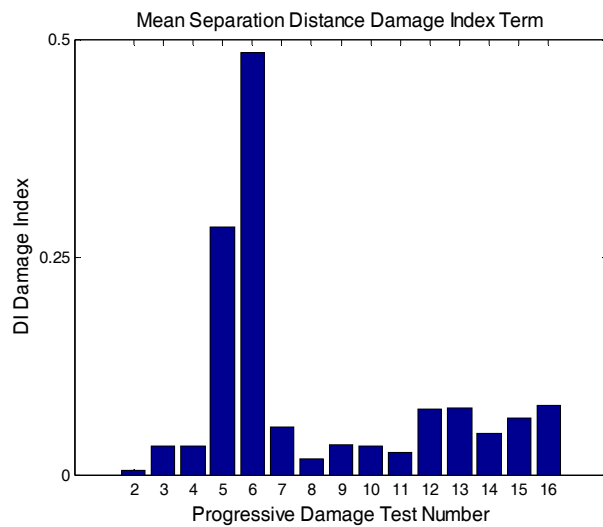


Figure 11(c): Damage index contributions from the mean separation distance criterion.

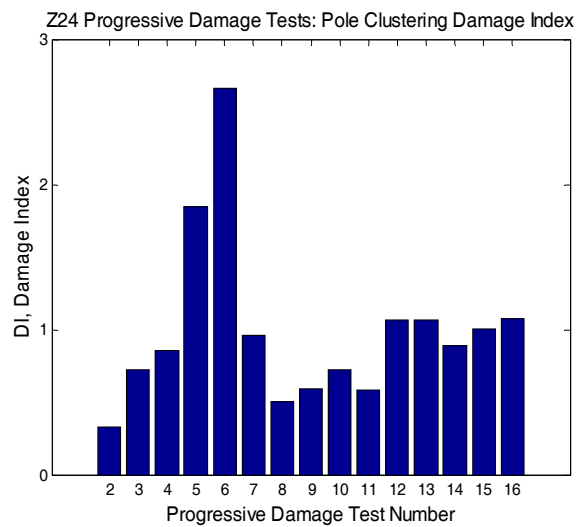


Figure 11(d): Final aggregated damage indices.

6. Acknowledgements

The authors would like to acknowledge the invaluable assistance provided by Dr. Helmut Wenzel of Vienna Consulting Engineers (Vienna, Austria). This work was funded by the National Science Foundation under Grant Number CMMI0726812 (Program Manager: Dr. S. Liu).

7. References

- [1] MnDOT, *Interstate 35W Mississippi River Bridge Fact Sheet*, <http://www.dot.state.mn.us/i35wbridge/pdfs/factsheet.pdf> (accessed on: October 11, 2007).
- [2] Rytter, A. "Vibration Based Inspection of Civil Engineering Structures," Ph. D. Dissertation, Dept. of Building Technology and Structural Engineering, Aalborg University, Denmark, 1993.
- [3] Doebling, S. W., Farrar, C. R., and Prime, M. R. "A Summary Review of Vibration-Based Damage Identification Methods," *Shock and Vibration Digest*, 30(2): 91-105, 1998.

- [4] Sohn, H., Farrar, C. R., Hemez, F. M., Shunk, D. D., Stinemates, D. W., Nadler, B. R., and Czarnecki, J. J., "A Review of Structural Health Monitoring Literature 1996-2001," Technical Report Annex to SAMCO Summer Academy, Los Alamos National Laboratory, Cambridge, 2003.
- [5] Celebi, M. "Seismic Instrumentation of Buildings (with emphasis on federal buildings)," Report No. 0-7460-68170, United States Geologic Survey (USGS), Menlo Park, CA, U.S.A., 2002.
- [6] Lynch, J. P., and Loh, K. "A Summary Review of Wireless Sensors and Sensor Networks for Structural Health Monitoring," *Shock and Vibration Digest*, 38(2):91-128, 2005.
- [7] Straser, E. G., Kiremidjian, A. S. (1998). "A modular, wireless damage monitoring system for structures," *Report No. 128, John A. Blume Earthquake Engineering Center*, Department of Civil and Environmental Engineering, Stanford University, Stanford, California.
- [8] De Roeck, G., Peeters, B., and Maeck, J. "Dynamic monitoring of civil engineering structures," *Proceedings of IASS-IACM 2000, Computational Methods for Shell and Spatial Structures, Chania, Greece*, 2000.
- [9] Krämer, C., De Smet, C. A. M., De Roeck, G. "Z24 bridge damage detection tests," *Proceedings of IMAC 17, the International Modal Analysis Conference, Kissimmee, FL, U.S.A.*: 1023-1029, 1999.
- [10] Peeters, B., and Ventura, C. E. "Comparative Study of Modal Analysis Techniques for Bridge Dynamic Characteristics," *Mechanical Systems and Signal Processing* 17(5): 965-988, 2002.
- [11] Womack, K., and Hodson, J. "System identification of the Z24 Swiss bridge," *Proceedings of IMAC 19, the International Modal Analysis Conference, Kissimmee, FL, U.S.A.*: 842-845, 2001.
- [12] Luscher, D. J., Brownjohn, J. M. W., Sohn, H., Farrar, C. R. "Modal parameter extraction of Z24 Bridge data," *Proceedings of IMAC 19, the International Modal Analysis Conference, Kissimmee, FL, U.S.A.*: 836-841, 2001.
- [13] Schwartz, B., and Richardson, M. "Post-processing ambient and forced response bridge data to obtain modal parameters," *Proceedings of IMAC 19, the International Modal Analysis Conference, Kissimmee, FL, U.S.A.*: 829-835, 2001.
- [14] Fassana, A., Garibaldi, L., Giorcelli, E., and Sabia, D. "Z24 Bridge dynamic data analysis by time domain methods," *Proceedings of IMAC 19, the International Modal Analysis Conference, Kissimmee, FL, U.S.A.*: 852-856, 2001.
- [15] Marchesiello, S., Piombo, B. A. D., and Sorrentino, S. "Application of the CVA-BR method to the Z24 Bridge vibration data," *Proceedings of IMAC 19, the International Modal Analysis Conference, Kissimmee, FL, U.S.A.*: 864-869, 2001.
- [16] Teughels, A., and De Roeck, G. "Structural Damage Identification of the Highway Bridge Z24 by FE Model Updating," *Journal of Sound and Vibration* 278: 589-610, 2004.
- [17] Garibaldi, L., Marchesiello, S., and Bonisoli, E. "Identification and Up-Dating Over the Z24 Benchmark," *Mechanical Systems and Signal Processing* 17(1): 153-161, 2003.
- [18] Kullaa, J. "Damage Detection of the Z24 Bridge Using Control Charts," *Mechanical Systems and Signal Processing* 17(1): 163-170, 2003.
- [19] Maeck, J., and De Roeck, G. "Damage Assessment Using Vibration Analysis on the Z24-Bridge," *Mechanical Systems and Signal Processing* 17(1): 133-142, 2003.
- [20] Mevel, L., Goursat, M. and Basseville, M. "Stochastic Subspace-Based Structural Identification and Damage Detection and Localisation-Application to the Z24 Bridge Benchmark," *Mechanical Systems and Signal Processing* 17(1): 143-151, 2003.
- [21] Lynch, J.P. "Linear Classification of System Poles for Structural Damage Detection using Piezoelectric Active Sensors," *SPIE 11th Annual International Symposium on Smart Structures and Materials*, San Diego, CA, U.S.A., 2004.
- [22] Lynch, J. P. "Damage Characterization of the IASC-ASCE Structural Health Monitoring Benchmark Structure by Transfer Function Pole Migration," *Proceedings of the 2005 ASCE Structures Congress*, New York, NY, U.S.A., 2005.
- [23] Ljung, L., *System Identification: Theory for the User, 2nd Edition*, Prentice Hall: Upper Saddle River, NJ, U.S.A., 1999.
- [24] Duda, R. O., Hart, P. E., and Stork, D. G. *Pattern Classification, 2nd Edition*, John Wiley and Sons: New York, NY, U.S.A., 2001.